

---

EFDA–JET–CP(07)03/41

M.P. Gryaznevich, T.C. Hender, D.F. Howell, L. Moreira, H. Reimerdes,  
Yu Baranov, C.D. Challis, J. Hobirk, A. Garofalo, S. Gerasimov, E. Joffrin,  
H.R. Koslowski, Y.Q. Liu, T. Luce, J. Mailloux, J. Menard, S. Saarelma,  
V. Pericoli, S D. Pinches, P de Vries and JET EFDA contributors

# Experimental Identification of the Beta Limit in JET

"This document is intended for publication in the open literature. It is made available on the understanding that it may not be further circulated and extracts or references may not be published prior to publication of the original when applicable, or without the consent of the Publications Officer, EFDA, Culham Science Centre, Abingdon, Oxon, OX14 3DB, UK."

"Enquiries about Copyright and reproduction should be addressed to the Publications Officer, EFDA, Culham Science Centre, Abingdon, Oxon, OX14 3DB, UK."

# Experimental Identification of the Beta Limit in JET

M.P. Gryaznevich<sup>1</sup>, T.C. Hender<sup>1</sup>, D.F. Howell<sup>1</sup>, L. Moreira<sup>1</sup>, H. Reimerdes<sup>2</sup>,  
Yu Baranov<sup>1</sup>, C.D. Challis<sup>1</sup>, J. Hobirk<sup>3</sup>, A. Garofalo<sup>2</sup>, S. Gerasimov<sup>1</sup>, E. Joffrin<sup>8</sup>,  
H.R. Koslowski<sup>4</sup>, Y.Q. Liu<sup>5</sup>, T. Luce<sup>2</sup>, J. Mailloux<sup>1</sup>, J. Menard<sup>6</sup>, S. Saarelma<sup>1</sup>,  
V. Pericoli<sup>7</sup>, S D. Pinches<sup>1</sup>, P de Vries<sup>1</sup> and JET EFDA contributors\*

<sup>1</sup>*Euratom/UKAEA Fusion Association, Culham Science Centre, Abingdon, Oxon, OX14 3DB, UK*

<sup>2</sup>*General Atomics, P.O.Box 85608, San Diego, CA 92186-5608, California, USA*

<sup>3</sup>*Max-Planck-Institut für Plasmaphysik, EURATOM-Assoziation, D-85748 Garching, Germany*

<sup>4</sup>*Forschungszentrum Juelich GmbH, EURATOM-Assoziation, D-52425 Juelich, Germany*

<sup>5</sup>*Association EURATOM-VR, Department of Applied Mechanics, Chalmers University of Technology,  
SE-41296 Gothenburg, Sweden*

<sup>6</sup>*Princeton Plasma Physics Laboratory, James Forrestal Campus, Princeton, NJ 08543, USA*

<sup>7</sup>*EURATOM-ENEA Association, C.R.Frascati, CP65, 00044 Frascati, Italy*

<sup>8</sup>*Association Euratom-CAE, DSM/DRFC, Cadarache F-13108, France*

*\* See annex of M.L. Watkins et al, "Overview of JET Results",  
(Proc. 21<sup>st</sup> IAEA Fusion Energy Conference, Chengdu, China (2006)).*

Preprint of Paper to be submitted for publication in Proceedings of the  
34th EPS Conference on Plasma Physics,  
(Warsaw, Poland 2nd - 6th July 2007)



Advanced tokamak regimes are associated with the increased normalised beta,  $\beta_N = \beta_t B_t a / I_p$  ( $\beta_t = 2\mu_0 \langle p \rangle / \beta_t^2$ ) and are often limited by MHD instabilities. Although the presence of an ideal conducting wall increases this beta limit, it is important to know the no-wall ideal b-limit as resistive wall modes can occur above this limit, which strongly depend on plasma rotation, current density profile, distance from the wall etc. It has been found that the Resonant Field Amplification (RFA) of an externally applied helical magnetic field is strongly enhanced when a plasma exceeds the ideal no-wall stability limit [1-3], so it can be used as an indication of a no-wall limit. This method of the no-wall limit identification has recently been routinely used in scenario development of high-beta discharges on JET.

RFA was studied on JET in three advanced regimes: the hybrid low-shear regime with  $q(0)$  close to 1, the high-beta low shear regime with  $1 \lesssim q(0) < 3.0$  and in a reversed shear ITB regime, by measuring the plasma response to externally applied AC helical magnetic fields, Fig.1. Here time dependences are shown of the plasma current, total NB power, normalised beta (blue), estimate of the no-wall limit (green, will be discussed below), amplitudes of  $n = 1$  (red) and  $n = 2$  (blue) modes (arbitrary values), EFCC current (black) and the plasma response component of  $B_r$  (red), which is an  $n = 1$  combination of midplane saddle loops in octants orthogonal to the applied perturbation and proportional to the RFA. In these experiments, four external Error Field Correction Coils (EFCC), Fig.2, were powered from two independent power supplies allowing application of a stationary  $n=1$  or 2 or a rotating  $n=1$  magnetic field. To measure the RFA, EFCC currents of 200 – 1000A ( $\times 16$  turns) have been used with frequency from 3Hz to as high as 60Hz, to increase the time resolution for the no-wall limit identification during fast increase in beta in some regimes. Either pair in EFCCs in Octants 1–5 or 3–7 was used to produce an  $n = 1$  field and the plasma response (vacuum field subtracted) was measured with combination of midplane in-vessel saddle loops in Octants 1, 3, 5 and 7. The induced perturbation was typically  $> 5$  times below the locked mode threshold and was not seen by any other diagnostics. The plasma response to the applied  $n = 1$  travelling waves with frequencies from  $\pm 3$ Hz to  $\pm 20$ Hz shows a distinct maximum at  $f \sim +3$ Hz (positive corresponds to rotation in the ion drift direction) and results were compared with an analytic model and MARS-F simulations [4] showing qualitative agreement.

The plasma response to a non-perturbative low-level  $n = 1$  stationary field shows a pronounced increase in the RFA at the no-wall limit in all three advanced regimes, as seen in the time evolution of the plasma response component of  $B_r$  in Fig.1. Fig.3 presents the dependence of the  $n = 1$  RFA on  $\beta_N$  in these three pulses, showing an increase indicating the no-wall limit. Here the RFA is determined as ratio of the plasma response to the applied vacuum field, which is close to the total RFA  $= (B_r - B_r^{\text{vac}}) / B_r^{\text{vac}}$  at beta values close to the no-wall limit. Typically, on JET, the RFA is seen well below the no-wall limit. RFA increases linearly with  $\beta_N$  until the no-wall limit is reached, when it will suddenly increase by factor 2–5. A precise identification of the no-wall ideal limit was complicated in some cases by presence of MHD activity. Fig. 4a shows non-monotonic increase in the  $n = 1$  RFA with clear increase in the RFA during the ELM-free period prior to the first ELM and correlation of

the maximum in the RFA with the first ELM, in high-beta low shear no-ITB Pulse No: 70199. This increase happens well below the identified no wall limit, Fig.4b. This also demonstrates a possibility of the first ELM prediction using the RFA in advanced regimes, which may be very important for mitigation of the non-acceptable large first ELM in ITER and other future fusion devices.

More than 130 pulses have been analysed using the RFA and the beta limit could be identified both during the beta rise and the beta fall caused by the MHD activity or by the end of the heating phase. Figure 5 shows evolution of the RFA with  $\beta_N$  during beta-rise and beta-fall periods in an ITB Pulse No: 70069 showing approximately the same limit in this case. Using this data it is possible to estimate the duration of the plasma sustainment over the no-wall beta limit. Fig.6 presents results of this analysis in different regimes. Here the maximum  $\beta$ -value is normalised on the average value of the no-wall limit between the  $\beta$ -ramp and  $\beta$ -fall. Each point represents a single pulse. In high- $\beta$  low shear no-ITB pulses (red), plasma with  $\beta_N \sim 1.2 \beta_N^{\text{no-wall}}$  can be sustained for up to 7 seconds, of the order of the characteristic time of current diffusion.

In the high- $\beta$  low shear (no-ITB) regime the time of the neutral beam injection was varied in order to achieve different values of the central q-value. A correlation between start time of NBI and reduction of the q(0) has been observed [5]. The dependence of the  $\beta_N^{\text{lim}}$  on the NBI time is shown in Fig.7, suggesting significant increase of the no-wall limit at lower q(0). It was also shown, that the no-wall limit dependence on the internal inductance ( $l_i$ ) can significantly vary from the commonly used  $\beta_N^{\text{lim}} \sim 4l_i$  scaling depending on the actual current profile. This is demonstrated in Fig.8, where evolution of the RFA with  $\beta_N/l_i$  in three high- $\beta$  low shear (no-ITB) pulses with different NBI start time and current ramp-up speed is shown. Vertical lines mark no-wall limits which varies from  $2.4l_i$  at high q(0), early NBI, to  $4.4l_i$  at low q(0), late NBI. This variation of the no-wall limit is shown in Fig.1, where the no-wall limit (green line in the second box) was estimated in different regimes using the RFA data.

The measured no-wall limit is in good agreement with MHD stability simulation using MISHKA [6] and MARS-F [4] codes. Fig.9 shows comparison of the no-wall limit measured in a no-ITB Pulse No: 68776 with MARS-F simulations (blue line) and MISHKA-F prediction based on calculations of the growth rate of an n = 1 mode in the absence of a wall (black line and green dots), both using experimental equilibrium for this regime.

These first tests of the use of the RFA as a routine diagnostics on JET show that it is a robust method of the no-wall limit identification. It has been shown that the no-wall limit on JET decreases with increasing q(0), as was predicted by the modelling [7]. This new diagnostics also allows to estimate duration of the plasma sustainment over the no-wall beta limit and it was shown that values of  $\beta_N \sim 20\%$  above the no-wall limit can be sustained on JET for up to 7 seconds, of the order of the characteristic time of current diffusion.

## ACKNOWLEDGEMENTS

This work was funded by the UK Engineering and Physical Sciences Research Council and by the

European Communities under the contract of Association between EURATOM and UKAEA. The views and opinions expressed herein do not necessarily reflect those of the European Commission.

## REFERENCES

- [1]. A. Garofalo et al, Phys. Plasmas **9**, 1997 (2002)
- [2]. A.H Boozer, Phys. Rev. Lett. **86**, 5059 (2001)
- [3]. H. Reimerdes et al, PRL **93**, 135002 (2004)
- [4]. Y.Q. Liu et al, Phys. Plasmas **13**, 056120 (2006)
- [5]. C.D. Challis et al, this conference.
- [6]. A.B. Mikhailovskii et al., Plasma Physics Reports, **23**, 884 (1997)
- [7]. J Menard, priv. communications

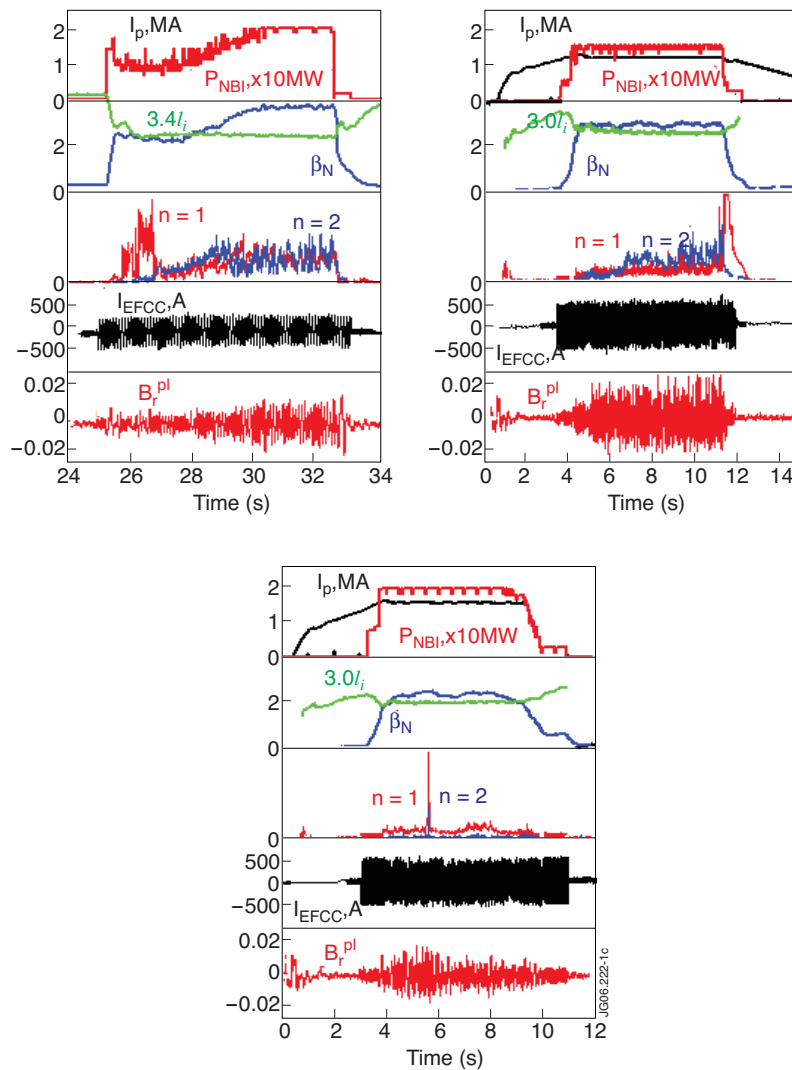


Figure 1: RFA in different JET scenarios: a - hybrid low-shear regime Pulse No: 69468,  $\beta$ -high- $\beta_N$  low shear (no ITB) regime 70254; c - reversed shear ITB regime 70322.

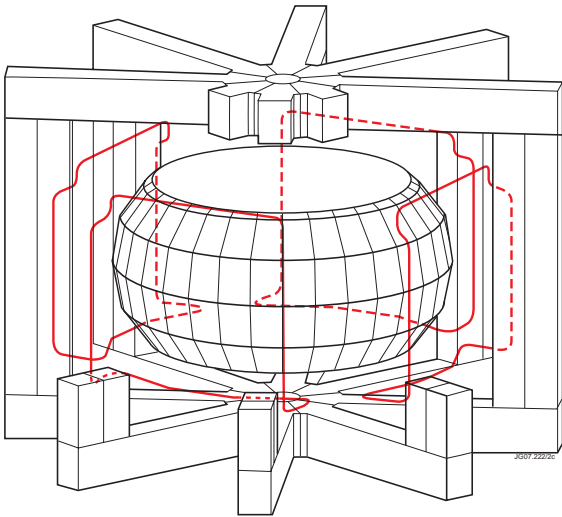


Figure 2: Schematic position of the external Error Field Correction Coils

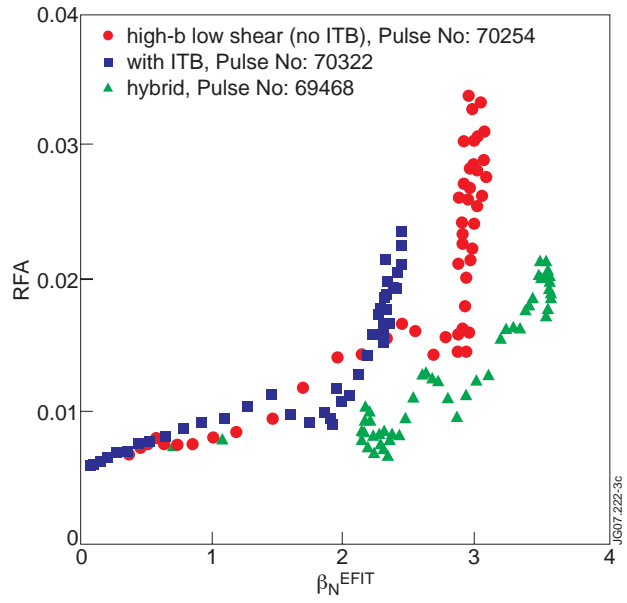


Figure 3: RFA evolution with  $\beta_N$  in different JET scenarios.

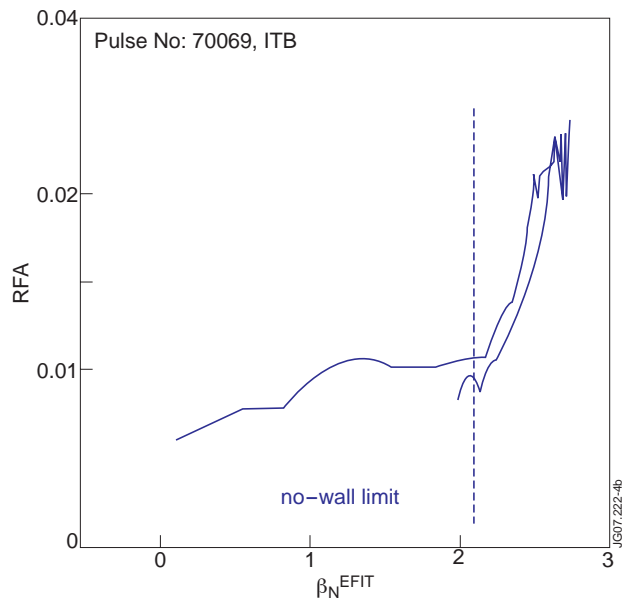
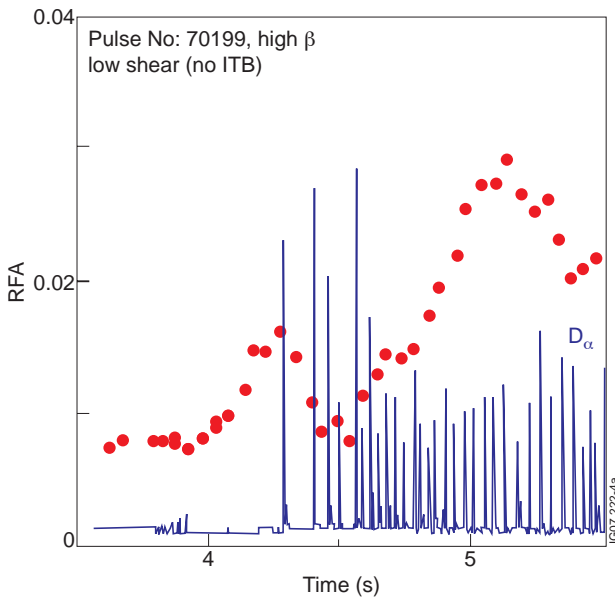


Figure 4:  $a-n=1$  RFA (red) and  $D_\alpha$  time traces,  $\beta_N n=1$  RFA evolution with  $\beta_N$ . Blue line shows no-wall limit.



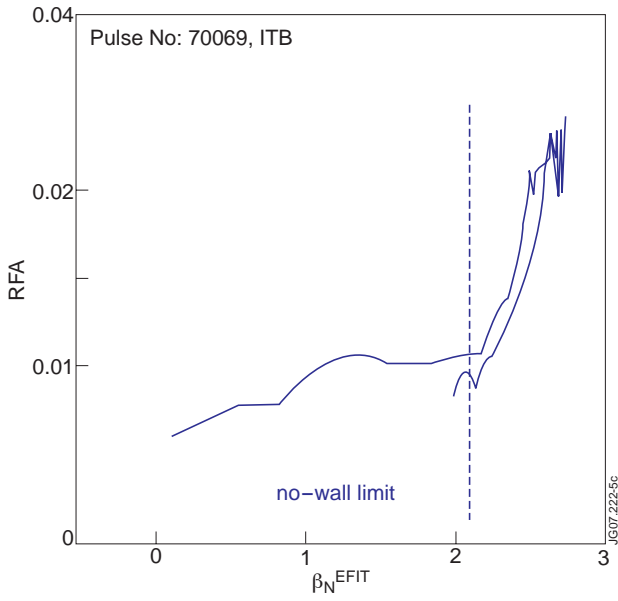


Figure 5: Evolution of the  $n=1$  RFA with  $\beta_N$  during beta-rise and beta-fall periods in ITB pulse.

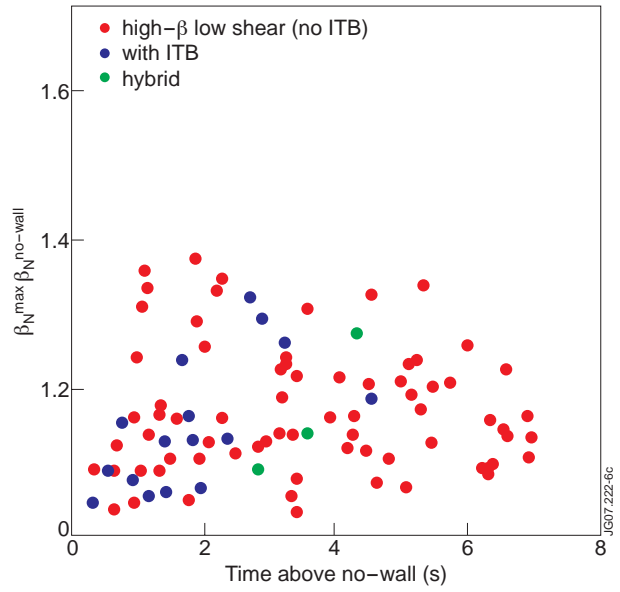


Figure 6: Ratio of maximum beta achieved in different JET scenarios to the no-wall limit.

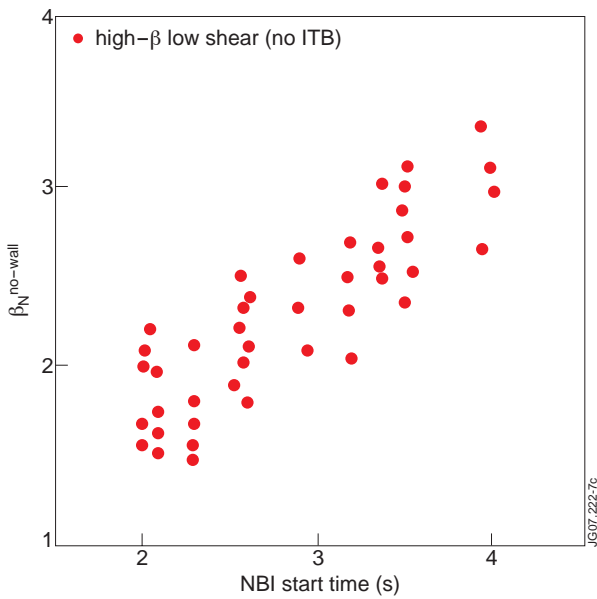


Figure 7: Dependence of the no-wall limit on the NBI application time in high-beta low shear no-ITB pulses

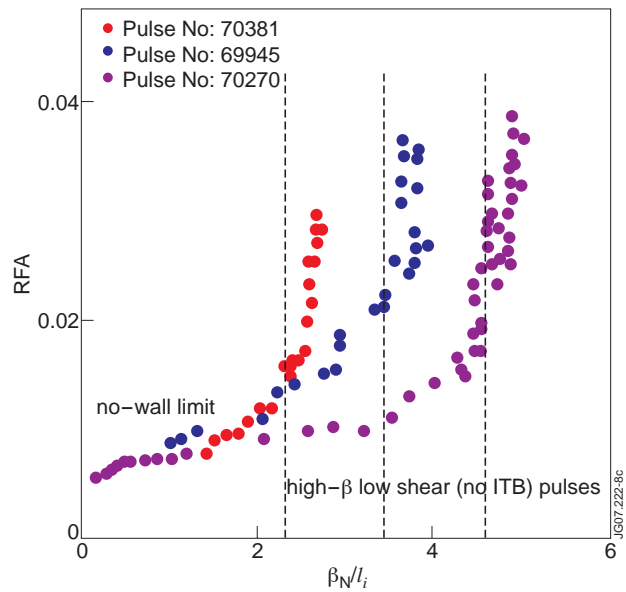


Figure 8: Evolution of the  $n=1$  RFA with  $\beta_N/l_i$  in three high-beta low shear no-ITB pulses

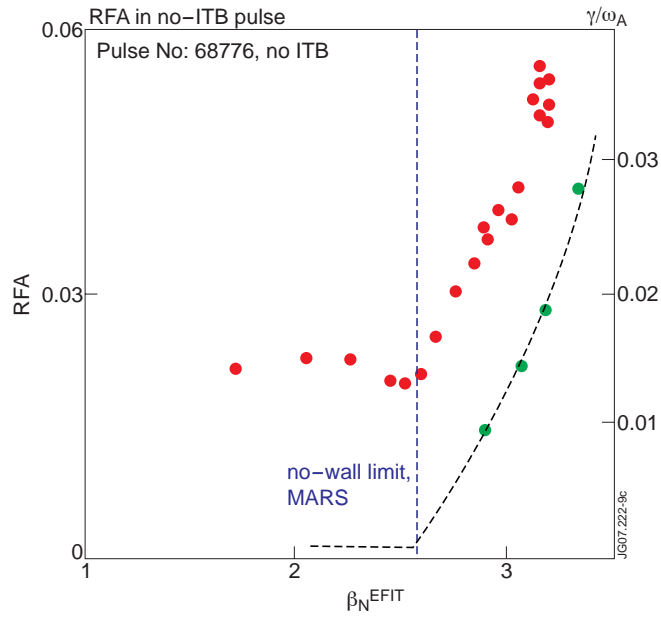


Figure 9: Comparison of the experimental no-wall limit with theoretical prediction: red – RFA data, blue line indicates the marginal- $\beta$  from MARS-F simulations for high- $\beta$  low shear (no ITB) regime, green dots – growth rate of the no-wall  $n=1$  mode calculated with MISHKA.